Displays 74 (2022) 102267

Contents lists available at ScienceDirect

Displays

journal homepage: www.elsevier.com/locate/displa

DSB-GAN: Generation of deep learning based synthetic biometric data☆

Pankaj Bamoriya [a], Gourav Siddhad [b], Harkeerat Kaur [c], Pritee Khanna [a,*], Aparajita Ojha [a]

[a] Department of Computer Science and Engineering, PDPM Indian Institute of Information Technology, Design and Manufacturing, Jabalpur, 482005, Madhya Pradesh, India
[b] Department of Computer Science and Engineering, Indian Institute of Technology, Roorkee, 247667, Uttarakhand, India
[c] Department of Computer Science and Engineering, Indian Institute of Technology, Jammu, 181221, Jammu & Kashmir, India

ARTICLE INFO

Keywords:
Autoencoder
Biometric
Data generation
Deep learning
GAN

ABSTRACT

Deep learning-based generative networks have brought a significant change in the generation of synthetic biometric data. Synthetic biometric data finds applications in developing biometric systems and testing them on a large amount of data to analyze their performance on extreme load scenarios or run simulation for health care personnel training. Generally, biometric datasets have fewer training samples, due to which deep learning models do not train well. In the proposed DSB-GAN, a generative model based on convolutional autoencoder (CAE) and generative adversarial network (GAN) is used to generate realistic synthetic biometrics for various modalities such as fingerprint, iris, and palmprint. This generated data ensures the availability of data that is not available in general due to various undesired factors like distortion and corruption of data. The model is resource efficient and generates diverse biometric samples as compared to state-of-the-art methods.

1. Introduction

Biometrics refers to the study of human biological characteristics that can be measured. Biometric technology is more accessible than ever before, bringing enhanced security and greater convenience to whatever needs protecting, from a door to a car or a smartphone. However, collecting biometric data is a time-consuming task and prone to distortion or corruption due to various factors such as lighting situation, position of the subject, camera resolution, sweat, dirt, and grease, etc. The real biometric data can be partially or entirely substituted with synthetic or simulated data to train biometric systems. This simulated or synthesized data is called synthetic biometric [1,2].

Synthetic biometric data can be extremely helpful in the case of data shortage for testing a biometric system. It can mitigate various issues faced in the collection of meaningful biometric data due to privacy concerns, deficiency of large biometric databases for evaluating biometric system performance on a large scale. For example, the contemporary automatic fingerprint synthesis addresses the problems of testing fingerprint identification systems, training security personnel, biometric database security, and protecting intellectual property [3]. Also, synthetic iris pattern has been used by ocularists in manufacturing glass eyes and contact lenses for a while. The ocularist's approach for synthetic iris is based on the composition of painted primitives and utilizes layered semi-transparent textures built from topological and optic models [4]. These methods are used today to create contact lenses with fake iris patterns printed onto them. Synthetic biometric data has applications in healthcare also [5]. It can be used for modeling at remote biomedical facilities to monitor patients' health in hospitals and care units. Simulation of various monitored data, as well as the extreme scenarios, helps healthcare personnel in decision making. The modeling and simulation of synthetic biometric data is used to provide efficient support for training security personnel in dealing with customer identification in physical access control systems [6].

The deep learning models have proved to be excellent feature extractors. However, the training of a deep learning network requires a large number of training samples [7]. Generally, biometric datasets have insufficient training samples (low number of subjects each having 5–20 samples per subject) which makes training of network difficult. A biometric based application deployed with a deep learning model poses a threat of adversarial attacks. Earlier also, the development of improved devices for human–computer interaction, enabling input of handwriting and signatures, called for the study of strategies for forging or generating synthetic signatures [8]. A large amount of data is needed for research to mitigate adversarial attacks. If the artificial/synthetic biometric data is properly created, it can be used for modeling a wide range of training neural networks, intrusion detection, spoofing, etc.

The proposed work aims to generate realistic synthetic biometrics that can be used to create large biometric datasets for the efficient training of deep learning networks. It can also be used to provide robustness

☆ This paper was recommended for publication by Guangtao Zhai.
* Corresponding author.
E-mail address: pkhanna@iiitdmj.ac.in (P. Khanna).

https://doi.org/10.1016/j.displa.2022.102267
Received 4 February 2022; Received in revised form 14 June 2022; Accepted 30 June 2022
Available online 5 July 2022

against adversarial attacks. The proposed deep leaning based synthetic biometric GAN (DSB-GAN) is based on a convolutional autoencoder (CAE) and DCGAN [9]. The proposed method is evaluated for three biometric modalities, fingerprint, iris, and palmprint. DSB-GAN has a low number of trainable parameters as compared to the state-of-the-art methods, which makes it efficient for real-time usage. The synthetic samples generated from this method are diverse and complete.

The rest of the paper is organized as follows. The following section discusses the related work done in this domain. Section 3 explains the methodology and experimental setup. Results are discussed in Section 4, and finally, the work is concluded in Section 5.

2. Literature review

The methods to generate synthetic biometric data can be classified into two categories: (a) Mathematical models (b) Deep learning models.

In mathematical models, the features from the biometric data are handcrafted manually. The data generation is done by manually extracting the base structure from one or more biometric samples. After this, various morphological modifications are performed and the synthetic biometric data is generated. SFinGe [10] is a method to generate artificial fingerprints based on mathematical models. SFinGe consists of four steps: (a) A specific geometric model is used for the construction of the shape of a fingerprint randomly; (b) Generation of a directional map; (c) Generation of a density map; and (d) A ridge flow model is used to construct the fingerprint pattern by combining all the three maps mentioned above. After this, some noise is introduced to make it natural. This method involves manual fine-tuning of the fingerprints and requires a lot of feature engineering. Also, this method is developed only for fingerprints. The mathematical models also suffer from generalization issues. Roy et al. [11] proposed the generation of the MasterPrint. The MasterPrint is generated by making some changes in the original biometric data. The resultant MasterPrint can fool a smaller biometric authentication system. The generated MasterPrint is of poor quality, due to which it is easy to differentiate between synthetic and original biometric data visually.

On the contrary to the handcrafted methods, the deep learning methods automatically extract features from the data. The development of generative networks has enabled the generation of high-quality data. Generative adversarial networks (GANs) has brought a significant change in the field of artificial intelligence [7]. The GAN fed with the input sample's data distribution generates synthetic data similar to the original input. But GAN suffers from various issues like unstable training, mode collapse, etc. Also, it is time and resource-exhaustive. To eradicate such problems, many variants of GANs were proposed. Most of these are based on DCGAN [9]. DCGAN differs from the simple GAN by the fact that DCGAN makes use of deep convolutional layers. DCGAN can be used to generate images of size 64×64. Some variants of DCGAN can generate images up to size 128×128. But it is unable to produce good results in the case of generating high-resolution data. To generate high-resolution images, Johnson et al. [12] proposed super-resolution, which reduces the computation expense for generating high-resolution data.

WGAN [13] proposed a loss function based on the Wasserstein distance or the earth mover distance. It also suggested weights clipping so that the Lipschitz conditions are fulfilled. But if a large parameter value is used for clipping, it can increase the network's time to converge. This can result in more complex training, the generation of bad quality images, and the non-convergence of the model. On the other hand, if a small parameter value is used for clipping, it can result in a gradient vanishing problem, especially for deep networks. WGAN-GP [14] proposed a penalty to be imposed on the gradient to fulfill the Lipschitz constraint to tackle this problem. In the discriminator network, batch normalization is not used. Otherwise, a correlation may occur across the batch samples, due to which the significance of penalizing gradient decreases. However, the use of this gradient penalty results in increasing the complexity of computation. Kodali et al. [15] proposed gradient update in an alternate manner which is useful when there is continuity in the original distribution of data and the generator distribution. This helps in the convergence of the network but is computationally expensive. Berthelot et al. [16] proposed BEGAN, to balance the generator and discriminator networks by using a loss based on the Wasserstein distance. The balancing of the generator and discriminator allows that none of the two can become more potent than the other. But this model suffers from a lack of diversity in the generated output.

DeepMasterPrint [17] proposed a GAN model based on Wasserstein distance and covariance matrix adaption evolutionary strategy to generate a master fingerprint, but this model could not produce sharp images. Minaee et al. proposed IrisGAN [18], FingerGAN [19], and PalmGAN [20] for the generation of synthetic iris, fingerprints, and palmprints, respectively. All these models are based on the DCGAN. In addition to DCGAN loss, FingerGAN and PalmGAN also use total variation loss. The generated results contain a large amount of noise and it takes a significant amount of time to train the models.

Shamsolmoali et al. [21] proposed G-GANISR to generate high-resolution data using the idea of super-resolution. Instead of using a single generator network, double generators were used. This helps in better training and makes the model robust. The loss function used for training the network is based on the least square method. The generated biometric data from this model suffer from a flawed structure and are blurred. Fahim and Jung [22] proposed a lightweight GAN Network for large-scale fingerprint generation (LGN-LSFG) that uses conditional loss doping and spectral normalization for stable training of the model. The model gives good results for fingerprint generation but does not perform well for palmprints and iris.

The methods discussed here have a large number of trainable parameters. Training these architectures is time-consuming and resource exhaustive. Also, most of these methods are not able to generate diverse and complete biometric samples. Therefore, a method is required that is time and resource efficient and can also generate diverse and complete biometric samples. The proposed method is targeted to fulfill both of these criteria.

3. Methodology

In the proposed deep leaning based synthetic biometric GAN (DSB-GAN), a CAE is trained to generate augmented data. This CAE is trained on biometric modalities such as fingerprint, palmprint, and iris for generating augmented data. Once trained, CAE generates biometric samples similar to the original biometric data, which can be used as augmented data for further training of neural networks. Using the generator from the DSB-GAN, artificial samples are generated. In the proposed method, augmented samples generated from the CAE, artificial samples from the generator, and the original biometric samples are combined together and fed to the discriminator to train the DSB-GAN. This augmented data increases the size of the training dataset, which adds to the better accuracy in generating biometric samples. This way, the synthetic biometric samples generated by DSB-GAN are similar to the original biometric samples, but diverse in nature. The flowchart of the proposed method is shown in Fig. 1. In comparison to other GANs, the proposed DSB-GAN is light-weight and uses original data as well as the augmented data generated from CAE for better training.

3.1. Proposed CAE

A CAE is proposed for data augmentation. The CAE consists of two networks, an encoder, and a decoder, as shown in Fig. 2. The encoder network consists of three convolution layers and two pooling layers. The number of filters used in convolution layers of the encoder is 32, 64, and 128, respectively. The pooling layers are used between the three convolution layers. The decoder network also consists of three convolution layers along with two upsampling layers. The number

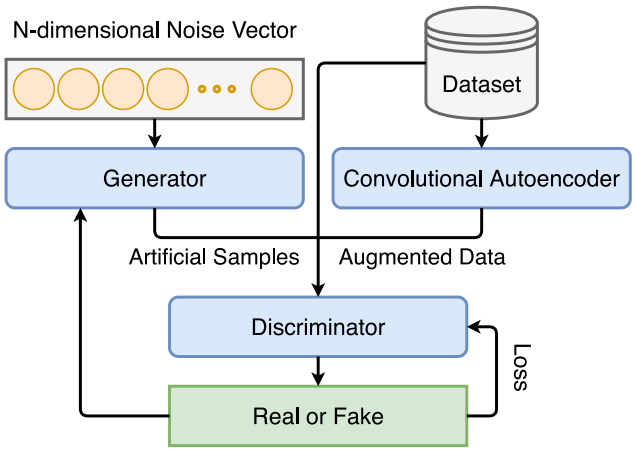

Fig. 1. Flowchart of the proposed methodology.

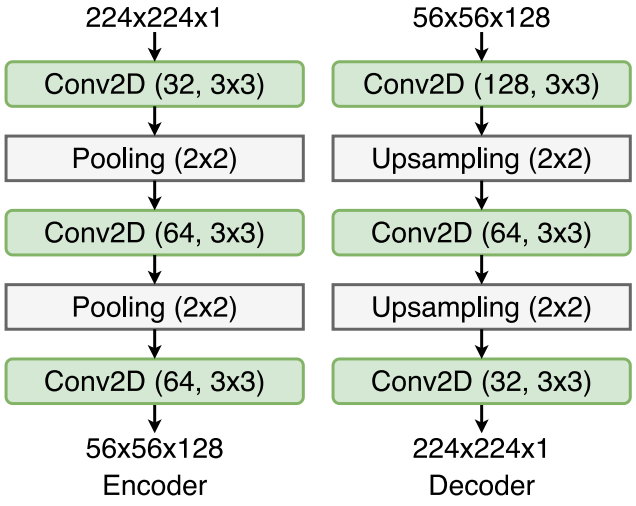

Fig. 2. Architecture of the CAE.

of filters used in convolution layers of the decoder is 128, 64, and 32, respectively. For each convolution layer, ReLU [23] is used as activation function. Similarly, two upsampling layers are used between the three convolution layers.

3.2. Proposed DSB-GAN

A deep leaning based synthetic biometric GAN (DSB-GAN) based on a deep convolution generative adversarial network (DCGAN) is proposed to generate biometric data. The proposed DSB-GAN model consists of two networks, a generator (Fig. 3) and a discriminator network (Fig. 3). Both the generator and discriminator networks are trained in an adversarial manner. It means that both the generator and discriminator networks try to maximize the other's loss and minimize its loss. An n-dimensional noise vector is given as input to the generator network. The generator network generates fake data samples. The generated artificial samples from the generator network and the augmented data samples from the CAE are combined together and shuffled to generate a large dataset. These samples are then given to the discriminator network of the DSB-GAN, which tries to distinguish between the real and fake samples. The generative model architecture enables it to capture the complex texture of input data, resulting in better model training. It allows DSB-GAN to produce good quality results.

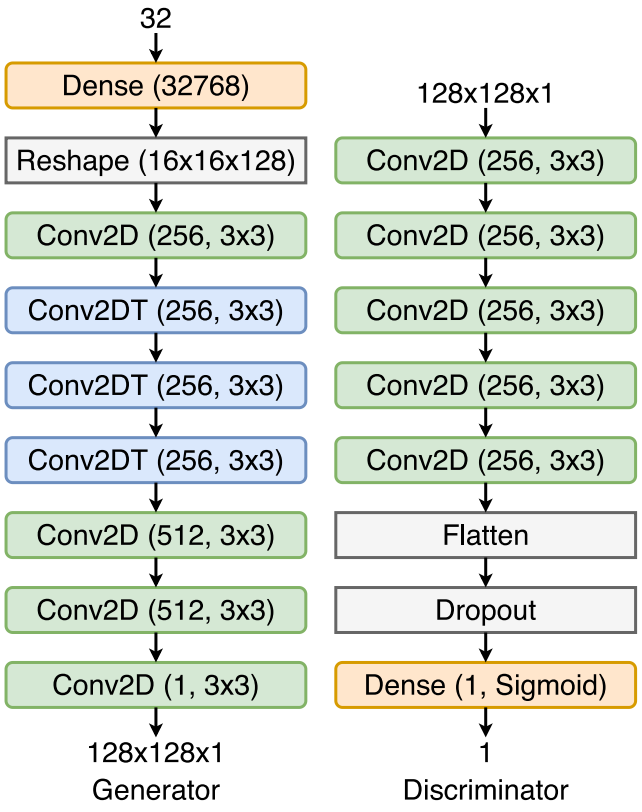

Fig. 3. Architecture of the DSB-GAN.

Table 1
Details of datasets used for experimentation.

Dataset	Subjects	Samples	Resolution	Images
IITD Iris [24]	224	5	320 × 240	1120
IITD Palmprint [25]	460	7	150 × 150	3220
PolyU Fingerprint [26]	300	6	328 × 356	1800
PolyU Palmprint [27]	400	20	384 × 284	8000

4. Results and discussion

4.1. Datasets used for experimentation

Four datasets of three biometric modalities are used for experimentation in this work. These datasets are PolyU fingerprint [26], PolyU palmprint [27], IITD iris [24], and IITD palmprint [25]. The description of these datasets is given in Table 1. The images are pre-processed before using for the experiment. The samples from these datasets are grayscale images with pixel values in the range of (0, 255) with a dimension of $H \times W$. To feed these samples to the CAE, the samples are reshaped to $H \times W \times 1$. These samples are then rescaled in the range of (0, 1). The dataset is now split into training and validation sets in a ratio of 80 : 20. Whereas, for feeding images as input to DSB-GAN, central crops are extracted from the original samples of size $H \times W$.

4.2. Parameters used for comparison

The proposed CAE model is evaluated in terms of mean squared error (MSE) [28], mean absolute error (MAE) [29], peak signal-to-noise ratio (PSNR) [30], and structural similarity index (SSIM) [31]. Here, MSE and MAE should be low and PSNR and SSIM should be high. These values denote that the images generated from the CAE do not have much variation and have high similarity to the input images.

Table 2
Performance of the proposed CAE.

Dataset	MSE	MAE	PSNR	SSIM
IITD Iris	0.0	0.02	68.27	0.83
IITD Palmprint	0.0	0.01	74.43	0.92
PolyU Fingerprint	0.0	0.03	59.17	0.38
PolyU Palmprint	0.0	0.01	78.41	0.94

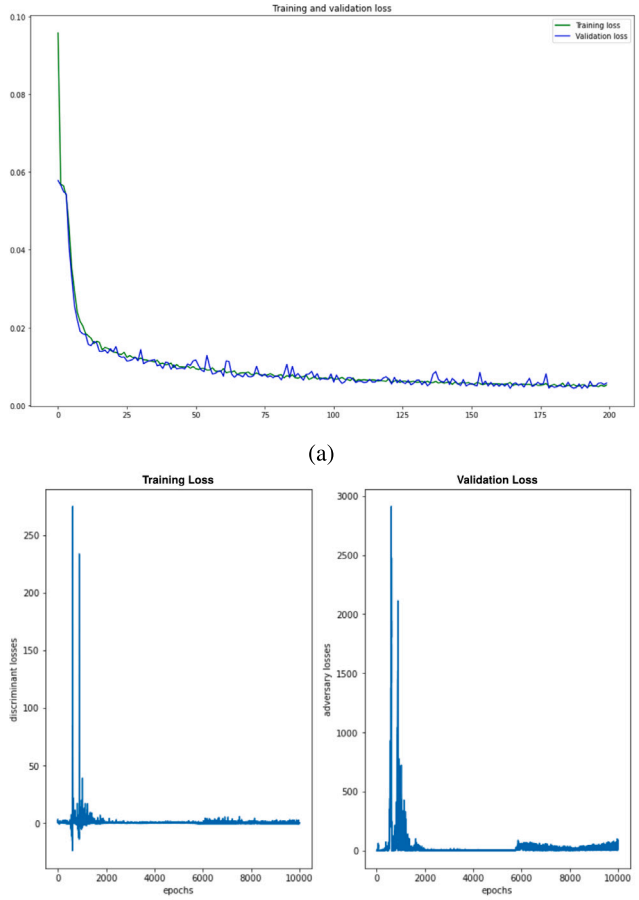

Fig. 4. Training and validation loss of (a) CAE and (b) DSB-GAN.

The performance of the DSB-GAN has been evaluated on two parameters, namely Fréchet inception distance (FID) [32] and multi-scale structural similarity index (MS-SSIM) [33]. FID is a metric used to evaluate the quality of the generated images. It was specifically developed for performance evaluation of GANs. FID has a range of [0, 100], where lower FID means smaller distances between synthetic and real data distributions. MS-SSIM is an advanced form of SSIM which is used to measure structural or perception information at various scales. It has a range of [0, 1] where 1 denotes perfect structural similarity. Low FID here means that the images generated are close to the original samples and low MS-SSIM denotes diversity and high variation between the samples generated by DSB-GAN.

4.3. Performance of CAE

The CAE has been trained for 200 epochs with a batch size of 128 and RMSProp [34] as the optimizer. Training and validation loss of CAE can be seen in Fig. 4(a). The proposed model is experimented on the four datasets mentioned in Table 1 for the generation of data.

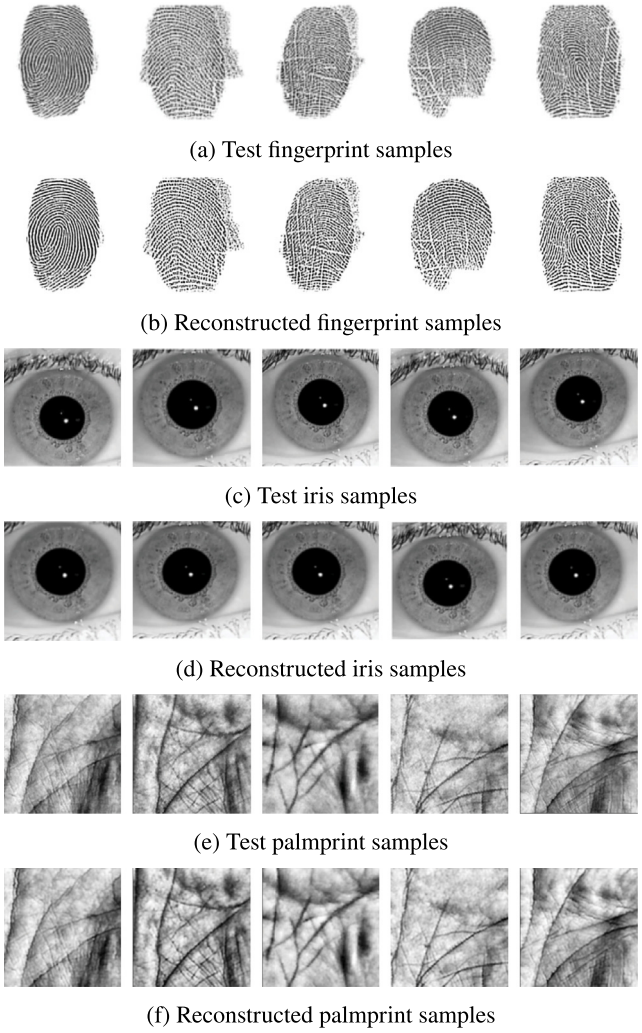

Fig. 5. Test and reconstructed samples from the CAE.

The proposed CAE model performed well. As depicted in Table 2, the proposed CAE has an MSE of 0, MAE in range (0.01–0.03) on the iris, palmprint, and fingerprint datasets used for experimentation. It can generate good-quality biometric data. MSE is 0 and MAE values are low for all four datasets. On the other hand, PSNR and SSIM values are high for all four datasets. These scores show low variation and high similarity between input and generated images. The test and reconstructed samples from the CAE can be seen in Fig. 5. It can be seen that the reconstructed images for all three modalities are clear and good quality. Figs. 5(a), 5(c), and 5(e) show the original fingerprint, iris, and palmprint samples from the datasets. Reconstructed fingerprints in Fig. 5(b), iris in Fig. 5(d), and palmprint in Fig. 5(f) indicate that the CAE model performs well and can reconstruct biometric data with good quality.

4.4. Performance of DSB-GAN

DSB-GAN has been trained for 10,000 steps with a batch size of 32 and RMSProp [34] as the optimizer. Training and validation loss of DSB-GAN can be seen in Fig. 4(b). The augmented data from the CAE is given to the proposed DSB-GAN for training and data generation. This data increases the overall training set size and helps better train the generative model. Some samples generated from DSB-GAN using fingerprint, iris, and palmprint datasets can be seen in Fig. 6. The generated artificial samples are shown in Fig. 6. The proposed model

Table 3
DSB-GAN as compared with other GANs in terms of quantitative parameters (at 95% confidence interval).

Method	#Param	FID			MS-SSIM		
		Fingerprint	Palmprint	Iris	Fingerprint	Palmprint	Iris
Finger-GAN [19]	40.5M	69.920 ± 4.020	52.892 ± 2.531	50.482 ± 2.127	0.693 ± 0.028	0.691 ± 0.015	0.566 ± 0.027
IrisGAN [18]	40.5M	71.848 ± 1.931	55.226 ± 1.931	40.956 ± 1.535	0.764 ± 0.020	0.676 ± 0.026	0.688 ± 0.018
PalmGAN [20]	40.7M	70.166 ± 1.368	40.086 ± 3.833	52.046 ± 1.686	0.708 ± 0.029	0.649 ± 0.028	0.594 ± 0.016
LGN-LSFG [22]	21.1M	47.392 ± 2.072	52.514 ± 1.808	46.906 ± 2.072	0.373 ± 0.022	0.658 ± 0.039	0.489 ± 0.021
DCGAN [9]	52.8M	74.990 ± 2.832	69.320 ± 3.119	72.772 ± 2.833	0.616 ± 0.029	0.748 ± 0.029	0.817 ± 0.020
BEGAN [16]	23.6M	52.524 ± 2.226	50.642 ± 1.403	64.328 ± 2.983	0.732 ± 0.028	0.570 ± 0.019	0.817 ± 0.022
WGAN [13]	58.7M	65.758 ± 2.666	69.264 ± 1.724	57.602 ± 2.870	0.446 ± 0.021	0.695 ± 0.018	0.653 ± 0.029
WGAN-GP [14]	58.7M	65.268 ± 2.417	67.568 ± 1.467	56.262 ± 3.120	0.434 ± 0.019	0.660 ± 0.025	0.610 ± 0.015
G-GANISR [21]	271.1M	49.902 ± 2.189	47.974 ± 1.574	50.764 ± 2.064	0.546 ± 0.019	0.466 ± 0.022	0.509 ± 0.019
Proposed DSB-GAN	**14.9M**	**39.992 ± 3.686**	**34.344 ± 5.614**	**34.182 ± 3.901**	**0.355 ± 0.104**	**0.360 ± 0.054**	**0.538 ± 0.047**

The first four GANs are specifically proposed for biometric data.

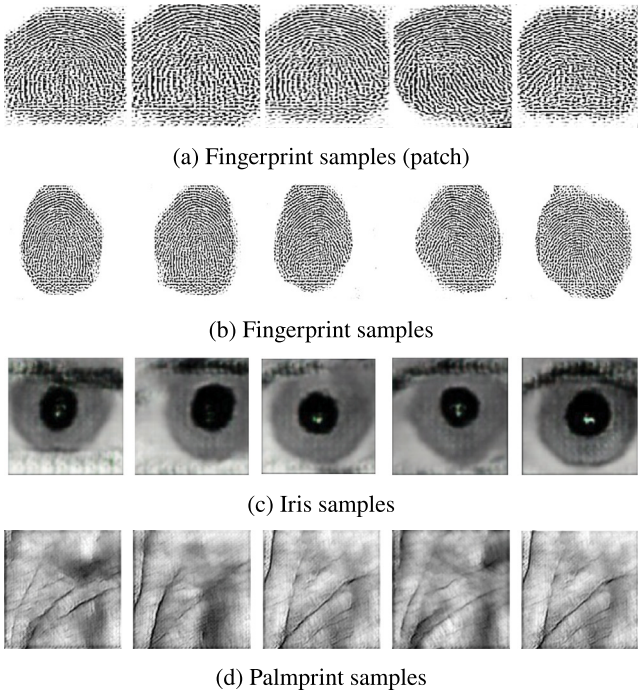

Fig. 6. Artificial samples generated by the proposed DSB-GAN: (a) fingerprint patch, (b) fingerprint, (c) iris, and (d) palmprint.

can be used to generate biometric image patches as well as complete images. Samples of fingerprints developed using the proposed model are shown in Fig. 6(b). Apart from fingerprint, the proposed model is used for the generation of artificial iris and palmprint data. Figs. 6(c) and 6(d) show the artificial iris and good-quality palmprint samples generated using the proposed model.

The performance of DSB-GAN is compared with various other GANs proposed in literature like DCGAN, BEGAN, WGAN, WGAN-GP, G-GANISR, LGN-LSFG, Finger-GAN, Palm-GAN, and Iris-GAN on FID and MS-SSIM scores. The details of these networks are given in Section 2. Table 3 contains comparative results based on quantitative evaluation. As discussed in Section 4.2, value of FID as well as MS-SSIM must be low to indicate that the distribution of images generated by DSB-GAN and original images are close to each other, while the generated images are diverse. The other methods have high value of FID which is not even close to DSB-GAN. MS-SSIM values for all methods are also high as compared to DSB-GAN. Both FID and MS-SSIM scores show that the images generated from DSB-GAN are diverse and have high variations among them. The proposed DSB-GAN has only 14.9M trainable parameters which are the lowest in comparison to those used in other GANs. This makes DSB-GAN light-weight and specific to biometrics. In case of the proposed DSB-GAN, output of CAE is also used as input to GAN, which is not done in other methods. In other methods only original data is used to feed the GAN, while in case of DSB-GAN, both original and augmented data are used to train the GAN. This helps DSB-GAN to achieve a better performance. Also, DSB-GAN is trained from scratch on biometric data along with the augmented data generated from the CAE, whereas other GANs are either not developed for biometric [9,13,14,16,21,22] or proposed for only a single biometric modality [18–20]. These networks were fine-tuned on biometric data that too on a single modality. The contribution of this work is a light-weight GAN to generate high quality and diverse biometric samples of various biometric modalities.

Fig. 7 shows the qualitative analysis with the different methods. It can be seen that the images generated from other methods are not able to generate clear images. Fingerprint and iris images generated from other GANs are unclear, and palmprint images are blurred. Also, fingerprint images are incomplete and texture is not visible in iris images. In comparison, the proposed DSB-GAN generates clear and complete images for all three modalities.

5. Conclusion

A DSB-GAN model based on CAE and DCGAN for the generation of high-quality biometric data is presented in this work. The proposed CAE model has minimal reconstruction error and a high SSIM score, which shows high similarity and low variation between the input and reconstructed biometric images. Therefore, the images reconstructed with CAE can be used for data augmentation. This step gives a large number of images for GAN input. The proposed DSB-GAN model can generate artificial biometric data for various modalities like fingerprint, palmprint, iris etc. The generated artificial samples from DSB-GAN are diverse and complete. The proposed DSB-GAN model has very few trainable parameters compared to other models, which makes it time and resource efficient.

CRediT authorship contribution statement

Pankaj Bamoriya: Methodology, Software, Investigation. **Gourav Siddhad:** Validation, Writing – original draft, Visualization. **Harkeerat Kaur:** Formal analysis. **Pritee Khanna:** Conceptualization, Resources, Validation, Writing – review & editing, Supervision. **Aparajita Ojha:** Writing – review & editing, Supervision.

Declaration of competing interest

The authors declare that they have no known competing financial interests or personal relationships that could have appeared to influence the work reported in this paper.

Data availability

The authors do not have permission to share data.

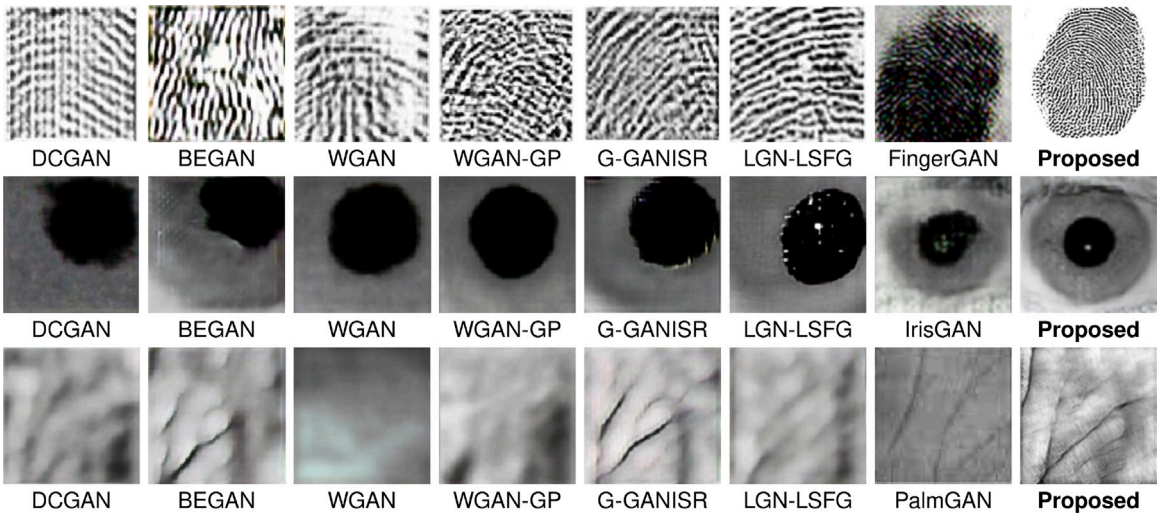

Fig. 7. Qualitative comparison on fingerprint (Row 1), iris (Row 2), and palmprint (Row 3) dataset.

References

[1] S.N. Yanushkevich, A. Stoica, V.P. Shmerko, D.V. Popel, Biometric Inverse Problems, CRC Press, 2018.

[2] S.N. Yanushkevich, A. Stoica, V.P. Shmerko, Developmental tools-synthetic biometrics, IEEE Comput. Intell. Mag. 2 (2) (2007) 60–69.

[3] D. Maltoni, D. Maio, A.K. Jain, S. Prabhakar, Handbook of Fingerprint Recognition, Springer Science & Business Media, 2009.

[4] A. Lefohn, B. Budge, P. Shirley, R. Caruso, E. Reinhard, An oculariste's approach to human iris synthesis, IEEE Comput. Graph. Appl. 23 (6) (2003) 70–75.

[5] K. Lai, S. Samoil, S. Yanushkevich, G. Collaud, Application of biometric technologies in biomedical systems, in: The 10th International Conference on Digital Technologies 2014, IEEE, 2014, pp. 207–216.

[6] S.N. Yanushkevich, Synthetic biometrics for training users of biometric and biomedical systems, in: 2011 International Conference on Cyberworlds, IEEE, 2011, pp. 5–8.

[7] I.J. Goodfellow, J. Pouget-Abadie, M. Mirza, B. Xu, D. Warde-Farley, S. Ozair, A. Courville, Y. Bengio, Generative adversarial networks, 2014, arXiv preprint arXiv:1406.2661.

[8] R. Plamondon, W. Guerfali, The generation of handwriting with delta-lognormal synergies, Biol. Cybernet. 78 (2) (1998) 119–132.

[9] A. Radford, L. Metz, S. Chintala, Unsupervised representation learning with deep convolutional generative adversarial networks, 2015, arXiv preprint arXiv:1511.06434.

[10] R. Cappelli, SFinGe: an approach to synthetic fingerprint generation, in: International Workshop on Biometric Technologies (BT2004), 2004, pp. 147–154.

[11] A. Roy, N. Memon, A. Ross, Masterprint: Exploring the vulnerability of partial fingerprint-based authentication systems, IEEE Trans. Inf. Forensics Secur. 12 (9) (2017) 2013–2025.

[12] J. Johnson, A. Alahi, L. Fei-Fei, Perceptual losses for real-time style transfer and super-resolution, in: European Conference on Computer Vision, Springer, 2016, pp. 694–711.

[13] M. Arjovsky, S. Chintala, L. Bottou, Wasserstein generative adversarial networks, in: International Conference on Machine Learning, PMLR, 2017, pp. 214–223.

[14] I. Gulrajani, F. Ahmed, M. Arjovsky, V. Dumoulin, A. Courville, Improved training of wasserstein gans, 2017, arXiv preprint arXiv:1704.00028.

[15] N. Kodali, J. Abernethy, J. Hays, Z. Kira, On convergence and stability of gans, 2017, arXiv preprint arXiv:1705.07215.

[16] D. Berthelot, T. Schumm, L. Metz, Began: Boundary equilibrium generative adversarial networks, 2017, arXiv preprint arXiv:1703.10717.

[17] P. Bontrager, A. Roy, J. Togelius, N. Memon, A. Ross, Deepmasterprints: Generating masterprints for dictionary attacks via latent variable evolution, in: 2018 IEEE 9th International Conference on Biometrics Theory, Applications and Systems (BTAS), IEEE, 2018, pp. 1–9.

[18] S. Minaee, A. Abdolrashidi, Iris-gan: Learning to generate realistic iris images using convolutional gan, 2018, arXiv preprint arXiv:1812.04822.

[19] S. Minaee, A. Abdolrashidi, Finger-GAN: Generating realistic fingerprint images using connectivity imposed GAN, 2018, arXiv e-prints. arXiv:1812.10482. arXiv:1812.10482.

[20] S. Minaee, M. Minaei, A. Abdolrashidi, Palm-GAN: Generating realistic palmprint images using total-variation regularized GAN, 2020, arXiv preprint arXiv:2003.10834.

[21] P. Shamsolmoali, M. Zareapoor, R. Wang, D.K. Jain, J. Yang, G-GANISR: Gradual generative adversarial network for image super resolution, Neurocomputing 366 (2019) 140–153.

[22] M.A.-N.I. Fahim, H.Y. Jung, A lightweight GAN network for large scale fingerprint generation, IEEE Access 8 (2020) 92918–92928.

[23] H. Ide, T. Kurita, Improvement of learning for CNN with ReLU activation by sparse regularization, in: Proceedings of the International Joint Conference on Neural Networks, Vol. 2017-May, 2017, pp. 2684–2691.

[24] A. Kumar, A. Passi, Comparison and combination of iris matchers for reliable personal authentication, Pattern Recognit. 43 (3) (2010) 1016–1026.

[25] A. Kumar, Incorporating cohort information for reliable palmprint authentication, in: 2008 Sixth Indian Conference on Computer Vision, Graphics & Image Processing, IEEE, 2008, pp. 583–590.

[26] C. Lin, A. Kumar, Matching contactless and contact-based conventional fingerprint images for biometrics identification, IEEE Trans. Image Process. 27 (4) (2018) 2008–2021.

[27] D. Zhang, Polyu Palmprint Database, Biometric Research Centre, Hong Kong Polytechnic University, 2006, (Online) Available from: (http://www.comp.polyu.edu.hk/biometrics/).

[28] Z. Wang, A.C. Bovik, Mean squared error: Love it or leave it? A new look at signal fidelity measures, IEEE Signal Process. Mag. 26 (1) (2009) 98–117.

[29] C. Sammut, G.I. Webb (Eds.), Mean absolute error, in: Encyclopedia of Machine Learning, Springer US, Boston, MA, 2010, p. 652, http://dx.doi.org/10.1007/978-0-387-30164-8_525.

[30] Q. Huynh-Thu, M. Ghanbari, Scope of validity of PSNR in image/video quality assessment, Electron. Lett. 44 (13) (2008) 800–801.

[31] Z. Wang, A.C. Bovik, H.R. Sheikh, E.P. Simoncelli, Image quality assessment: from error visibility to structural similarity, IEEE Trans. Image Process. 13 (4) (2004) 600–612.

[32] M. Heusel, H. Ramsauer, T. Unterthiner, B. Nessler, S. Hochreiter, Gans trained by a two time-scale update rule converge to a local nash equilibrium, Adv. Neural Inf. Process. Syst. 30 (2017).

[33] Z. Wang, E.P. Simoncelli, A.C. Bovik, Multiscale structural similarity for image quality assessment, in: The Thrity-Seventh Asilomar Conference on Signals, Systems & Computers, 2003, Vol. 2, Ieee, 2003, pp. 1398–1402.

[34] G. Hinton, Neural networks for machine learning; Lecture 6a - Overview of mini-batch gradient descent, 2010, Available at http://www.cs.toronto.edu/~tijmen/csc321/slides/lecture_slides_lec6.pdf.